4PP9A Honours Year Project

An investigation into the use of photo-diodes for the readout of a cosmic ray telescope which could be used in schools and a study of a small Hamamatsu photo-multiplier as an alternative. This project also briefly investigates the combinations of scintillator, wavelength shifter and waveguides for the optimum readout performance.

Paul Laycock

1 Introduction

1.1 An Outline of the Cosmic Schools Group Project

The idea behind the Cosmic Schools Group Project is to install in a school a cosmic ray telescope, as shown in figure 1, which is capable of being operated within that school. The long term objective is to install these detectors in as many schools as possible around the country, thereby making, with the help of the Global Positioning Satellite, a large cosmic ray telescope array.

The detector consists of a nine by nine array of scintillators (bottom) and a single central scintillator (top), providing directional information. The dimensions of these individual plastic scintillator sheets is expected to be 30 $\times$ 30 cm^2 and the distance between the top and bottom layers is about two metres.

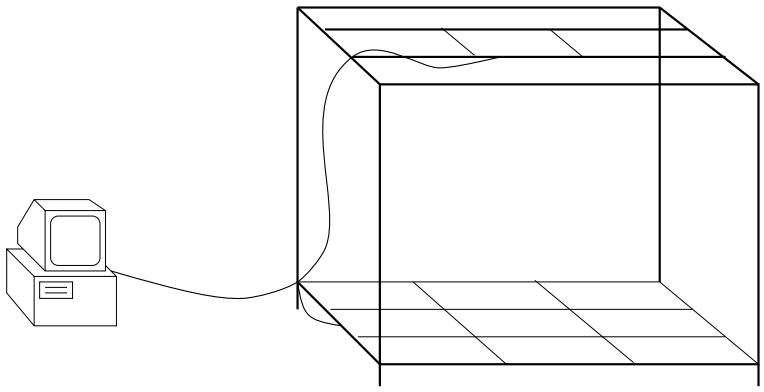

Figure 1: Schematic illustration of the apparatus for one element of the Cosmic Schools Group Detector

1.2 An Outline of this Project

The cost of this project is of great importance, as the aim is to install each school with one detector. The ease of operation and upkeep is also an important consideration, although the fact that detectors of this kind can be operated within schools has already been demonstrated by one of the members of the Cosmic Schools Group.

The main bulk of this project will be to determine the readout method for the scintillators. There are two options to be considered here, the first of which is the use of a photo-diode. These are relatively cheap and would greatly reduce the cost of the detector as a whole, remembering that ten

readout devices are needed per detector. The second readout method available is the use of a new small photo-multiplier manufactured by Hamamatsu. These devices incorporate an HV system making them safe for use in schools.

I shall also briefly look at the means of delivering the scintillation light from the scintillator to the photon detection device (photo-diode or photo-multiplier). A common method is to use a strip of wavelength shifter and attach the device to the small face of this. I shall make a preliminary study of the effect of using wavelength shifter in this situation.

2 Photon production and Detection

2.1 Photon production in an inorganic scintillator

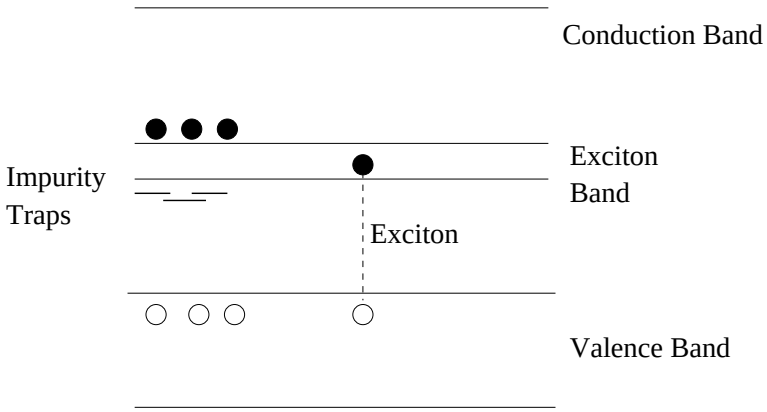

Figure 2: Scintillation mechanism for an Inorganic scintillator

An exciton is formed upon the absorption of a photon and this exciton migrates through the crystal. The exciton is then captured at an impurity site where it de-excites, thereby emitting radiation. In the case of the Caesium Iodide scintillator which I have used, Thallium has been added to create more of these impurity sites making CsI(Tl) which is a more efficient scintillator.

The reason for using CsI(Tl) is that it has a higher light output than the plastic scintillator. It is useful then for setting up the system as fixed-energy gamma-ray sources will deposit all of their energy in a block of CsI(Tl), allowing an energy calibration. It also presents the best chance of 'seeing' cosmic rays and provides a yardstick as to where we should expect to see the cosmic ray signal from a plastic scintillator.

2.2 Photon production in a plastic scintillator

Plastic scintillators are made by dissolving an organic scintillator in a plastic solvent. In organic scintillators the scintillation light arises from transitions made by the free valence electrons. These electrons are de-localised and occupy molecular orbitals (called π orbitals).

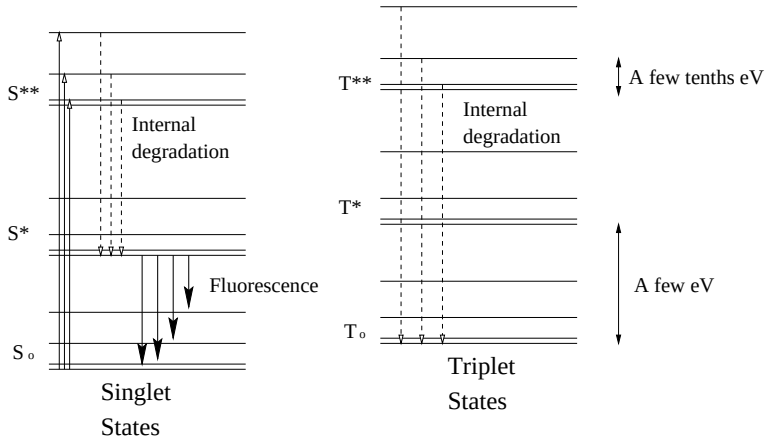

Figure 3: Scintillation mechanism for an Organic scintillator

Internal degradation to the S$\star$ state is (generally) immediate and radiationless. Within a few ns the electron will then decay from the S$\star$ state to the S$\circ$ vibrational state, emitting radiation. The Triplet states behave similarly; internal degradation occurs to the T$\circ$ state which decays mainly by

$$\mathrm{T}\circ + \mathrm{T}\circ \rightarrow \mathrm{S}\star + \mathrm{S}\circ + \text{phonons}$$

Consequent de-excitation of S$\star$ emits radiation as before. This process takes longer and is thus called the slow component. The slow component is only significant in some materials.

Plastic scintillators are suggested for the Cosmic Schools Group Project because they are cheap and can be readily machined into the desired size and shape. The scintillator is readily available in the form of 1 cm thick sheets.

2.3 Photo-multipliers

The following is only intended to a very brief and basic description of the operation of a photo-multiplier. A copy of the H5784 specifications is included as an Appendix.

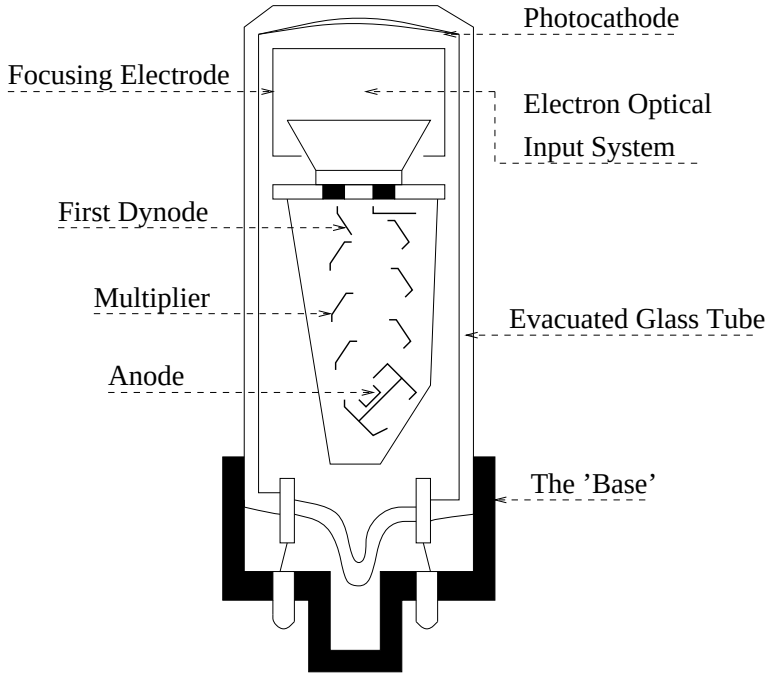

Figure 4: Schematic Illustration of a Photo-multiplier

The incident photon hits the photo-cathode which emits an electron by the photo-electric effect. An applied voltage accelerates the electron to the first dynode where some of its energy is transferred to the electrons in the dynode; secondary electrons are emitted. The applied voltage accelerates these electrons towards the second dynode, where yet more electrons are emitted, and so on. An electron cascade is formed down the dynode string until it is collected at the anode to give a current which can be amplified and analysed.

2.4 Photo-diodes

For the sake of brevity I will describe only the simplest view of how a P-i-N junction can be used as a photon detector.

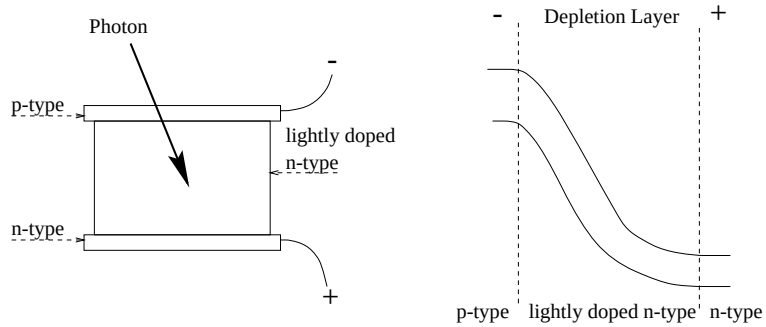

(a.) (b.)

Figure 5: (a.)Schematic Illustration of a P-i-N junction and (b.) Plot of Voltage Vs Position to demonstrate the high junction field in the depletion layer

The energy difference between the bottom of the conduction band and the top of the valence band for Silicon is 3·6 eV. For photons with an energy $h\nu \geq E_{gap}$ one electron-hole pair is formed for each photon absorbed. Carriers generated in the depletion layer will separate in the high junction field, giving a current flow from n to p , i,e, in the reverse direction. The SiN surface on the photo-diode I used gives rise to a better quantum efficiency of the photo-diode.

Note that $h\nu \geq E_{gap}$ is sufficient to create an electron-hole pair as the photon momentum is small.

2.5 Wavelength shifters

Wavelength shifters are used to match the quantum efficiency of a detector to the wavelength of the incident light. Again the wavelength shifting material is dissolved in a plastic solvent which means that it is very easy to use and durable. The wavelength shifter (WLS) absorbs light from a plastic scintillator at $\lambda \simeq 420$ nm and then re-emits light, isotropically, at $\lambda \simeq 480$ nm. The WLS is usually available in the form of strips which can be attached to one edge of a scintillator sheet. The readout device can then be attached to the small face of this strip, ensuring a high collection efficiency at that face.

3 Calculations of Light yield

The calculations in this section are intended to give only a rough estimate of the signal to noise ratios I can expect to see. It is necessary to make several assumptions along the way, although these are hopefully justified.

The first task is to calculate the fraction of light we can expect to collect at the readout face.

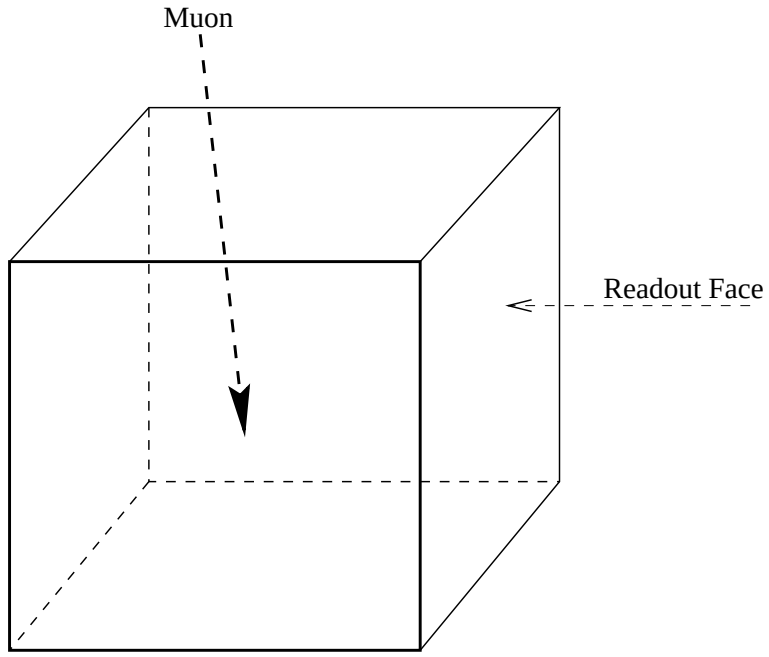

Figure 6: A cube modelling the CsI(Tl) crystal

I assume that there is no preferential direction for the light to travel and so the readout face will receive one sixth of the available light. In order to reach that face I assume that the light will have collided with the surface of the crystal (wrapped with reflector) on average three times. I further assume that the fraction of light reflected at each collision is one ninth. The fraction of light incident on the readout face, ϵ_S is then given by:

$$\frac{1}{6} \times \frac{9}{10} \times \frac{9}{10} \times \frac{9}{10} \simeq 0 \cdot 1$$

where I have rounded down as the detector does not cover the full readout surface. I expect that this fraction is an underestimate in the case of the (approximately) cubic CsI(Tl) block, but it should be fair in the case of the plastic scintillator sheet.

Important properties of the scintillation materials to consider are:

Property	CsI(Tl)	Plastic
Density (g cm^{-3})	4.51	1.032
λ_{max} (nm)	580	420
Light Output (%)	95	60
Decay constant (ns)	1100	2-3
Refractive Index	1.788	1.58

Table 1: Properties of the Scintillators

3.1 CsI(Tl) scintillator coupled with the Hamamatsu photo-multiplier

The quantum efficiency, ϵ_{HPM}, for the Hamamatsu photo-multiplier (HPM) at a wavelength of 580 nm is approximately 0·04. The scintillation light output of CsI(Tl) is 16000 photons per MeV. The energy deposited in the CsI(Tl) block that I am using is given by the depth of the block, the density of the block and the energy loss of muons in the block. To a good approximation the muons will travel vertically through the block. The thickness of the block I measured to be 7·5 cm, the density as given in table 1 is 4·51 grams per cm (in one dimension) and the commonly quoted figure for muon energy loss in matter is 2 MeV per gram. The energy deposited is then:

$$\begin{aligned} Energy &= 7.5cm \times 4.53gcm^{-1} \times 2MeVg^{-1} \\ &= 67.65MeV \end{aligned}$$

This means that approximately 1·08 $\times$ 10^6 photons are produced in the CsI(Tl) block every time a cosmic ray travels through. The number of photo-electrons I expect to collect with the HPM is given by:

$$\begin{aligned} Photons\,Detected &= Photons\,Produced \times \epsilon_S \times \epsilon_{HPM} \\ &= 4330\,photoelectrons \end{aligned}$$

which is the number of photo-electrons produced by the photo-cathode. These are then amplified by the dynode chain and an estimate of the amplification of the HPM is $3{\times}10^5$. This gives an estimate of the number of signal photo-electrons as:

$1.299{\times}10^9$ Photo-electrons

3.2 CsI(Tl) scintillator coupled with a photo-diode

Having performed the calculation for the HPM it is then a simple matter to replace ϵ_{HPM} with the quantum efficiency of the photo-diode at 580 nm. The photo-diode is actually more efficient than the HPM, with $\epsilon_{PD} = 0{\cdot}85$. The number of photo-electrons produced by the photo-diode per cosmic ray is simply:

$$\begin{aligned} Photons\,Detected &= 1.08 \times 10^6 \times 0.1 \times 0.85 \\ &= 92000\,photoelectrons \end{aligned}$$

This is the figure I will use as a signal to noise reference as it is the amplification process that produces the noise.

3.3 Plastic scintillator coupled with the photo-multiplier

The plastic sheets of scintillator are not cubic at all, but much flatter. I therefore expect ϵ_s to be a fair estimate of the fraction of light arriving at the readout face. According to figures from an experiment at DESY a 1 cm thick piece of scintillator produces 15000 photons with an incident cosmic ray. The quantum efficiency, ϵ_{HPM}, of the HPM at 420 nm is approximately 0·25. The HPM photo-cathode should then yield:

$$\begin{aligned} Photons\,Detected &= 15000 \times 0.1 \times 0.25 \\ &= 375\,photoelectrons \end{aligned}$$

Again using an amplification factor of $3{\times}10^5$ this means that at the anode there will be:

$1.125{\times}10^8$ photo-electrons

3.4 Plastic scintillator coupled with a photo-diode

The quantum efficiency of the photo-diode at 420 nm is $\epsilon_{PD} = 0{\cdot}6$. The number of photo-electrons produced by the photo-diode will be:

$$\begin{aligned} Photons\,Detected &= 15000 \times 0.1 \times 0.6 \\ &= 900\,photoelectrons \end{aligned}$$

Again this is the figure I shall use to calculate the signal to noise ratio.

3.5 Signal to Noise Ratio Calculations

For the sake of simplicity and for convenience I will use a commonly quoted figure for the noise of 1000 photo-electrons.

The signal to noise ratio (SNR) for the HPM on CsI(Tl) is:

$$\begin{aligned} SNR &= \frac{1.299 \times 10^9}{1000} \\ &= 1.299 \times 10^6 \end{aligned}$$

There should be no difficulty in seeing the cosmic ray signal from the CsI(Tl) using the HPM.

The SNR for the photo-diode on CsI(Tl) is:

$$\begin{aligned} SNR &= \frac{92000}{1000} \\ &= 92 \end{aligned}$$

There should be no problem in seeing the cosmic ray signal from the CsI(Tl) using the photo-diode.

The SNR for the HPM on the plastic scintillator is:

$$\begin{aligned} SNR &= \frac{1.125 \times 10^8}{1000} \\ &= 1.125 \times 10^5 \end{aligned}$$

Again there should be no problem seeing the cosmic ray signal from the plastic scintillator using the HPM.

The SNR for the photo-diode on the plastic scintillator is :

$$\begin{aligned} SNR &= \frac{900}{1000} \\ &= 0.9 \end{aligned}$$

I do expect there to be some difficulties in using the photo-diode on the plastic scintillator, especially as the noise factor for the photo-diode can dramatically increase depending on the conditions.

4 Experimental Setup

4.1 A Simple Cosmic Ray Telescope

The first task I had to perform was to construct a simple cosmic ray telescope which I could then use to test and compare the efficiency of the two detectors. There were several scintillator-waveguide sections available in the lab and, after finding two good photo-multipliers, I could use these to build my telescope.

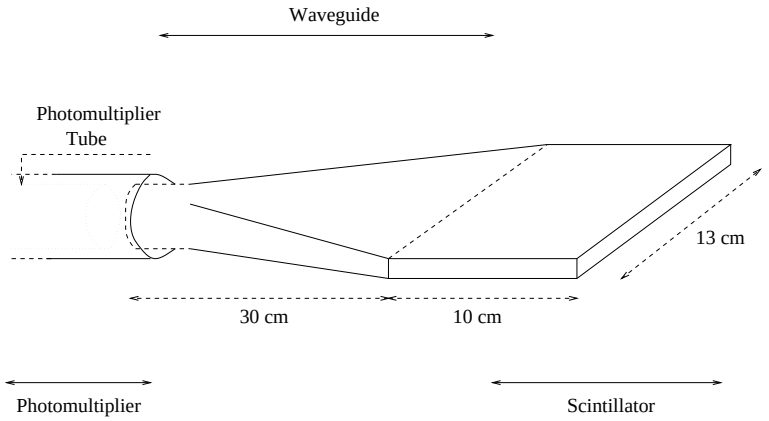

Figure 7: Illustration of a scintillator-waveguide section

The simplest method of making a telescope is to place the two scintillators, read out by the photo-multipliers (PM's), one on top of the other, separated by some arbitrary distance. To achieve a high count rate I used a separation of approximately 7 cm (this was the separation set by the photo-multiplier stand). A simple logic operation can then be used to determine when the two PM's produce a signal simultaneously, i.e. when a cosmic ray has passed through both scintillators.

4.1.1 Discriminators

The discriminator is used to eliminate much of the low-level noise which is inherent in most photo-multipliers. The threshold is set manually ,by means of a screw, to be just below the level of the required signal strength. In leading-edge triggering the output signal is generated as soon as the input level exceeds the threshold. The output signal is in the form of a logic pulse.

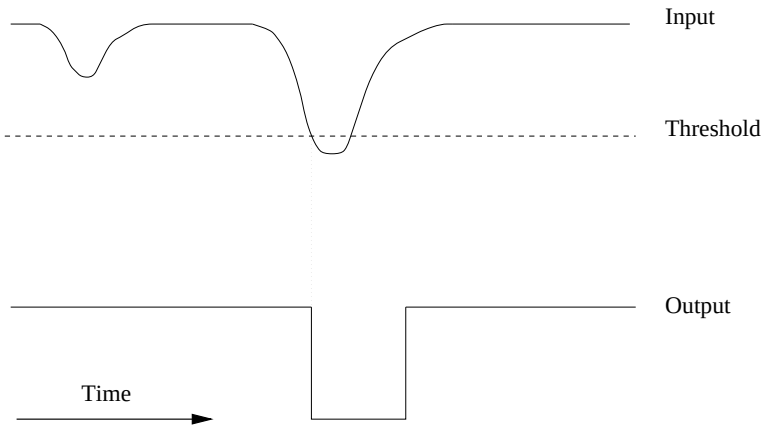

Figure 8: Illustration of the function of a Discriminator

4.1.2 Coincidence Counters

This device simple sums the two inputs and compares it to a threshold, again set manually by a screw. A 'coincidence' occurs, i.e. an output pulse is generated, when the two input signals are close enough in time to overlap.

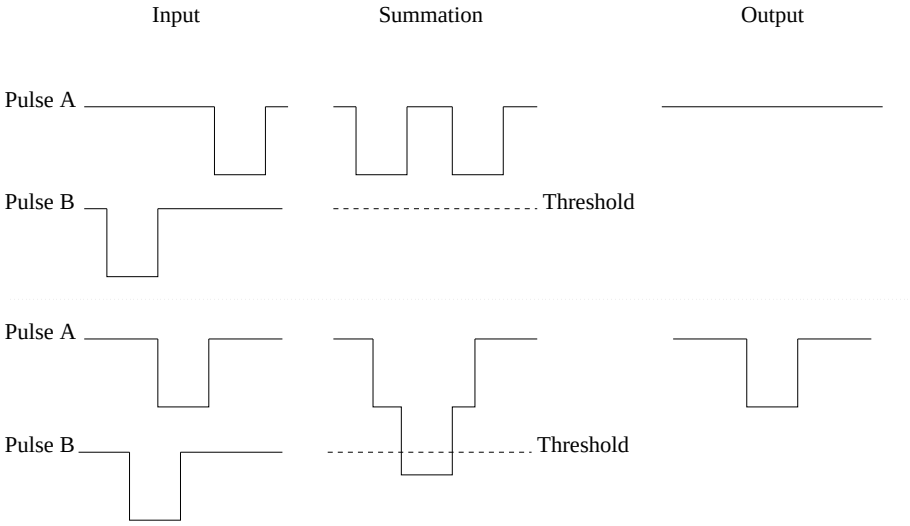

Figure 9: Illustration of the function of a Coincidence Counter

4.1.3 Pulse Generator

This simply allows manipulation of the final output signal pulse from the telescope. Among the variables this allows are the output voltage, the pulse width (in μs) and the pulse delay time (again in μs or longer). This facility proved crucial in proving that the signal on the spectrum is due to cosmic rays and is not some other effect, e.g. the electronics.

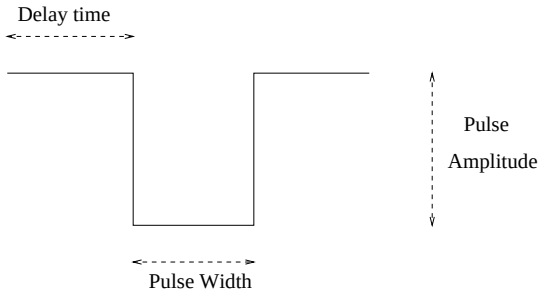

Figure 10: The three variables of concern for this project

During the experiment (see Figure 11) these values were set at:

- Delay Time = Zero Delay
- Pulse Width = 15 μs
- Pulse Amplitude = 6 V

4.1.4 A Multi-Channel Analyser

The MCA digitises a signal using an Analogue to Digital Converter (ADC).The Multi-Channel Analyser (MCA) sorts incoming pulses according to pulse height. The number of pulses in each height bin is then recorded in a multi-channel memory. Finally the channels and their number of entries can be graphically represented in the form of a histogram, which I will refer to as a spectrum of the data.

The package I used had two inputs, the Normal Input and the Coincidence Input. The Normal Input works in the manner described above. The Coincidence Input is used to tell the Normal Input when to switch on and how long for by using a gate pulse, which is the end product of the telescope output (Pulse Generator signal). As the gate pulse is 15 μs wide the delay time caused by the different lengths of cables, of the order of ns, does not have any effect. **Note** that the 15 μs gate pulse is used as, with the brief assistance of a digital oscilloscope, I was able to confirm that this width covered the photo-diode pulse.

4.2 Cosmic Ray Detection with a Photo-diode

I now have a comic ray telescope which provides an output pulse every time a cosmic ray passes through both scintillators. The rate at which these pulses are produced (or flux of cosmic rays) is on average about one per second. I can therefore ignore (at least for the time being) random coincidences generated by the PM's.

I can now proceed with the first part of this project, as I have done it, which is to use the photo-diode as a detector. I simply need to affix the photo-diode to the Scintillator using one of the several possible methods (see Section 5). Placing the Scintillator between the two telescope scintillators means that every time the telescope records a pulse I expect to see a pulse from the photo-diode. The telescope is used to generate a gate for the photo-diode which is fed into the MCA along with the photo-diode output. Every time a gate is generated by the telescope, the MCA records the output of the photo-diode.

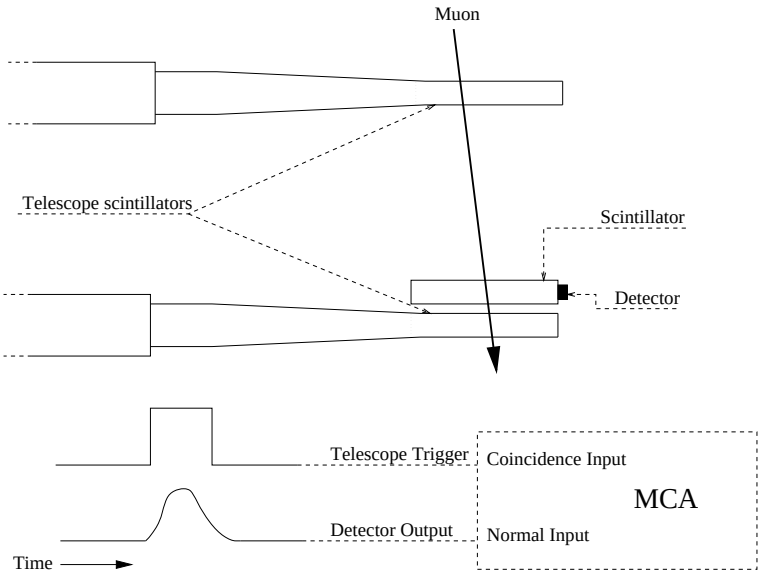

Figure 11: Method of measuring the efficiency of a detector

4.2.1 Pre-amplifier

The weak signal generated by the photo-diode needs to be collected and amplified as soon as possible to keep a good signal to noise ratio. The pre-amplifier is connected via a low noise cable (length approximately 15 cm)

to the photo-diode to reduce capacitance and 'pick-up' noise. The charge-sensitive pre-amplifier integrates the charge carried by the pulse on the capacitor C_f. The output voltage does not depend on the capacitance of the detector and is proportional to the charge collected by the detector.

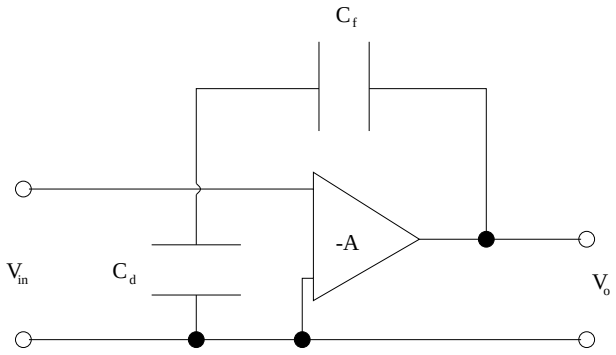

Figure 12: Circuit diagram of a Charge-sensitive Pre-amplifier

4.2.2 Spectroscopic Amplifier

This device performs two main tasks:

1. Amplification of the signal from the pre-amplifier
2. Shaping of the signal into a convenient form for further processing

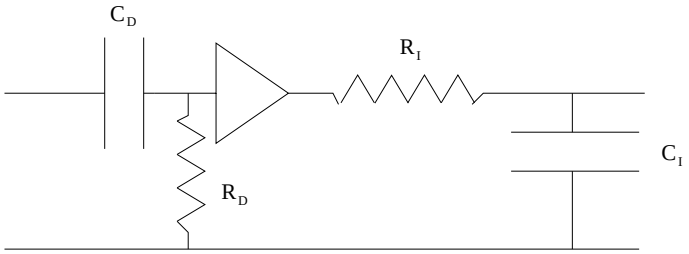

Figure 13: Illustration of the form of a circuit diagram for a spectroscopic amplifier

The pulse from the pre-amplifier generally has a long exponential tail, which can last between a few and 100 μs. When a second signal arrives 'on' this tail its amplitude will be enhanced. Further signals arriving on successive tails results in a phenomenon known as 'pile-up', destroying the information being collected.

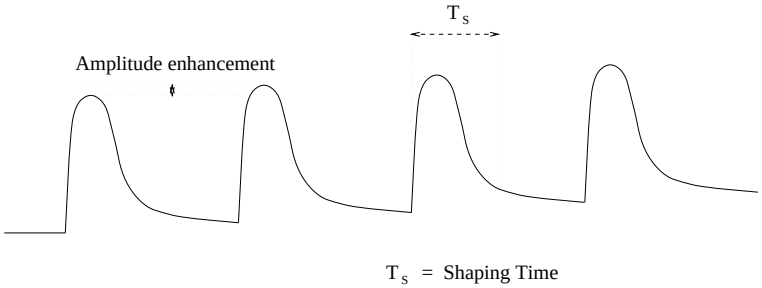

Figure 14: The 'Pile-up' phenomenon

The spectroscopic amplifier crops the signal after a time called the shaping time (selected via a knob on the unit), given by:

$$T_S \quad = \quad R_D \times C_D = R_I \times C_I$$

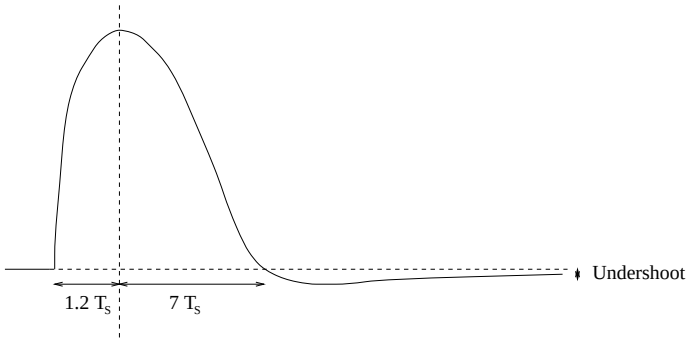

Figure 15: Output signal of the Spectroscopic Amplifier

The output signal of the amplifier now looks something like Figure 15. The undershoot only returns very slowly to zero, so if a signal were to arrive on top of this undershoot there would be an amplitude defect. The solution to this problem is called Pole-Zero cancellation and once again it is adjusted via a screw on the unit.

The signal can then be fed into the Multi-Channel Analyser.

Note that an added benefit of passing the signal through the circuit shown in Figure 13 is that the signal to noise ratio is improved. This is because the CR-differentiator circuit acts as a filter at low frequencies, while the RC-integrator circuit acts as a filter at high frequencies. I will not include any theoretical support for this here.

4.2.3 Earthing and Noise

The photo-diode I used, a Hamamatsu 2744-08, was originally required to read out a CsI(Tl) crystal for use in a calorimeter (to be used in the BaBar experiment). The reliability and noise performance of the photo-diode are crucial for this experiment and so I assume that their Set-up parameters for the pre-amplifier and spectroscopic amplifier are as close to optimum as possible. I adopted these parameters thanks to the assistance of Dr. Gerd Dahlinger in the preliminary stages.

The remaining problem is to ensure that the photo-diode is adequately shielded and that pick-up is minimised. This again involved the advice of Dr. Gerd Dahlinger and I implemented the following precautions:

1. The apparatus, up to and including the pre-amplifier, are contained in a light tight Aluminium box.

2. The minimum-ionising block and aluminium foil wrapping for the scintillator were given a common earth.

3. The entire apparatus is separated from any other apparatus or experiment and is powered, in series, from a single power point.

4. All possible noise sources, e.g. monitors, are kept as far as possible from the apparatus and are used for as little time as possible.

An easy method to 'see' the noise level and achieve a quick estimate for comparison is to view the noise pedestal. This is done by directly reading out the photo-diode using the MCA and produces in a few seconds a sharp peak that falls away exponentially. Looking at the highest channel into which this noise pedestal pervades gives a useful 'measure' of the noise conditions. Finding the 'best' channel then allows for reproducibility, as when the apparatus is dis-connected, re-arranged and then re-connected an inspection of the noise pedestal gives the current noise conditions.

Note that to actually achieve the 'best' conditions again takes some time and patience, or as Dr. Gerd Dahlinger put it 'It's Magic!'. However, the technique does allow for some confidence in the reproducibility of the results and was particularly useful for finding bad connections and noise sources, although finding the bad connection is another matter.

4.2.4 Minimum Ionizing Particles

There is another consideration to ensure that the cosmic ray signal is as well-defined as possible and therefore gives as resolved a signal as possible. It is necessary to ensure that only minimum-ionising particles are detected by the telescope. These are particles whose energy loss is at, or is near, the minimum, i.e. the particles do not stop in the second scintillator. A lead block, later replaced by a copper block ($\sim$1 cm thick), was placed between the two telescope scintillators for this purpose (labelled M.I.B. in Figure 16 for Minimum Ionizing Block).

4.2.5 The Photo-diode Set-up

In the schematic illustration of Figure 16 I have, for convenience, abbreviated the two telescope scintillator-waveguide sections and their respective photo-multipliers to simply 'Photomultiplier A' and 'Photomultiplier B'. The reader should also note that 'Input 1', used by the photo-diode, is the input which can be read directly (see Section 4.2.3) by the MCA in the computer.

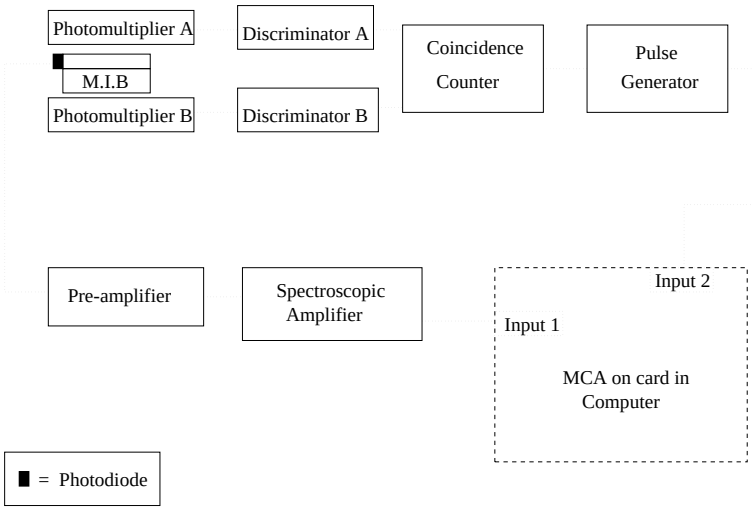

Figure 16: Schematic Illustration of the Photo-diode Set-up

4.3 Cosmic Ray Detection with the Hamamatsu Photo-multiplier

In comparison with the photo-diode the H5784 Hamamatsu photo-multiplier is easier to use. A pre-amplifier is included within the housing as well as an integrated HV circuit, so the pick-up is greatly reduced. The H5784 can be affixed to the scintillator and then, if required, put through a spectroscopic amplifier.

4.4 Data Analysis

4.4.1 Spectra produced by the MCA

The spectra produced by the MCA are represented as a histogram. The software permits some basic manipulation of the data, such as expansion of particular regions of interest and comparison with another spectrum. However, to be able to fit the spectra properly it is necessary to export the data, in CSV format, to another program, namely PAW++.

4.4.2 Fitting with PAW++

The spectra produced in this experiment are somewhat more complicated than might be expected and so attempts to fit entire spectra all failed. In the case of some spectra which appeared to be convolutions of a Gaussian peak on an exponential background (both of which can be fitted using PAW++ routines) all attempts to fit the data failed. Fortunately for the purposes of this experiment a Gaussian fit of the peak is sufficient to determine a good estimate of the peak position.

Other spectra appeared to be more complicated convolutions of a Landau distribution with a resolution determined by the Gaussian distribution. An approximation for the Landau formula:

$$
\begin{aligned}
y &= \frac{e^{[-(\lambda+e^{-\lambda})/2]}}{\sqrt{2\pi}} \\
with & \\
\lambda &= R(E - E_P) \\
E_P &= most\ probable\ energy\ loss \\
R &= Constant\ defined\ by\ absorber
\end{aligned}
$$

was used in a simple Fortran programme, along with the Gaussian formula:

$$G = e^{\frac{-(X_i - X)}{2\sigma^2}}$$

to find values for the most probable energy loss, i.e. the peak position.

A plot of the program with arbitrary values showed that it produced the correct form of curve. Unfortunately though the programme proved to be extremely sensitive to the range being fitted and the fit proved to be very poor. PAW++ produces, upon displaying the fitted data, the smooth line fit that it has calculated. This smooth line, although it did possess the correct form, did not fit the data at all accurately. In particular it did not match the curvature of the data and the peak position calculated was far too sensitive to the range of the fit.

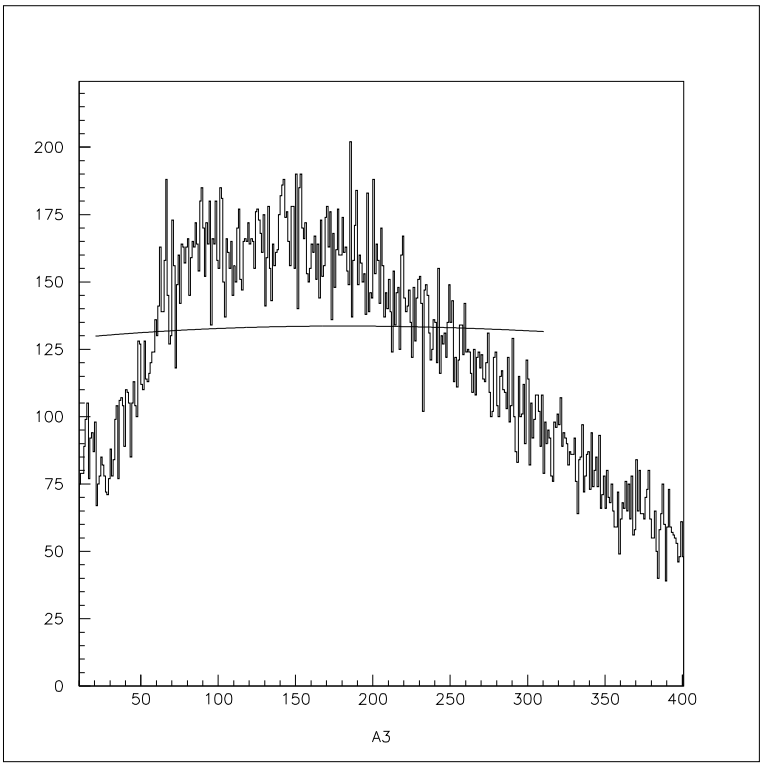

Figure 17: The 'best' fit achieved using the Landau Fortran program

Once again though a simple Gaussian fit of the peak provided a reasonable estimate of the peak position for the purposes of this experiment.

5 Combinations

I include here an aside on the wrapping of the scintillators. As I have previously mentioned in Section 4.2.3 an experiment involving the readout of CsI(Tl) crystals is already well established and I have adopted much of the wrapping precautions from Dr. Gerd Dahlinger. I have chosen to use one layer of reflective wrapping, the most available being aluminium foil. An air gap between the scintillator and wrapping increases the chances of total internal reflection and hence increases the light output.

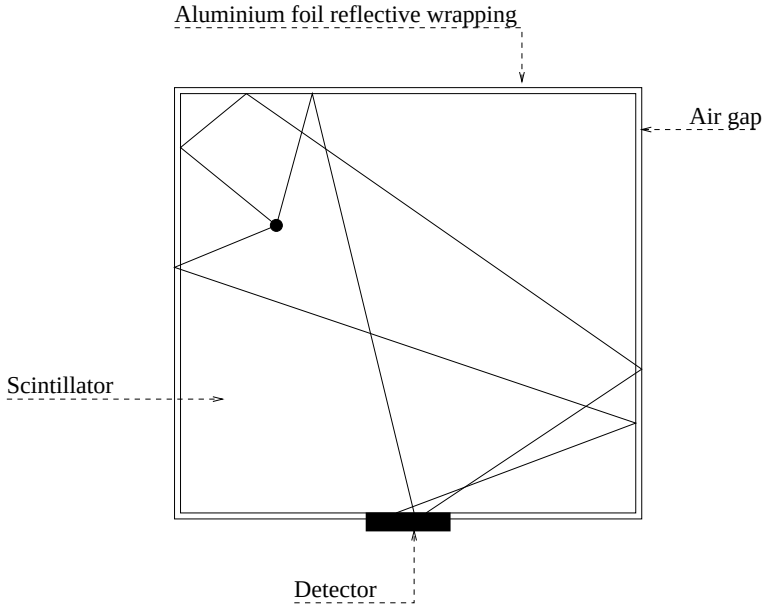

Figure 18: Schematic Illustration of the wrapped scintillator

Not shown in Figure 18 is another well-used method of keeping the scintillator light-tight; wrapping the whole scintillator, along with the aluminium, waveguide and detector, with black tape plumbing tape). Again care must be taken when applying the tape to ensure that there is an air gap between the scintillator and its wrapping.

5.1 Direct readout from the scintillator

During the preliminary stages of the experiment, whilst trying to 'find' the cosmic ray signal, I used this method with a piece of scintillator of the same dimensions as the telescope scintillators (10 cm by 13 cm). This provided the best chance of seeing a signal as there is as little loss as possible (no

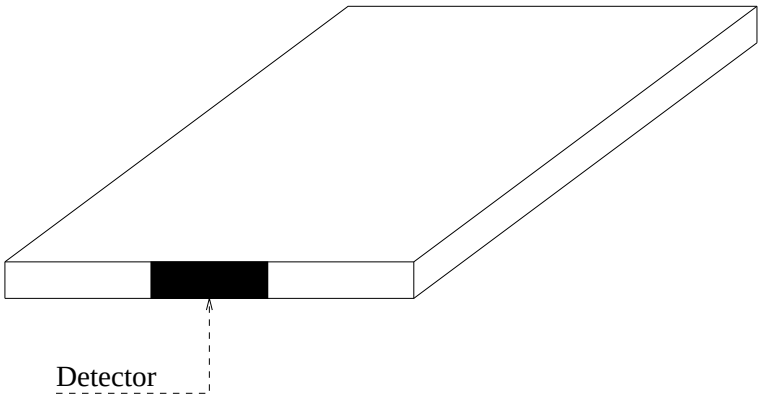

Figure 19: The Direct readout method

connections to waveguides, etc.). Using a detector Scintillator with the same dimensions as the telescope scintillators also means that nearly all (as many as possible) of the signals generated in the detector Scintillator will have generated a coincidence count by the telescope. There is also the more obvious benefit of a greater collection efficiency of the detector on a smaller piece of scintillator.

Note that the photo-diode is placed on the smaller edge (10 cm) to obtain a greater ratio of area coverage. It is affixed to the scintillator using Silicon grease as an optical coupling.

5.2 Readout with a waveguide

A great deal of care is needed to glue a piece of scintillator to a waveguide to ensure that there are no air bubbles in the joint. Air bubbles decrease the light output by 'trapping' light but in reality and in laboratory conditions it is almost impossible to create a glue joint without air bubbles. The waveguide is also wrapped with aluminium reflector and black tape (care being taken to ensure that there are no gaps). The light should be attenuated down the waveguide so a decrease in light output and hence resolution is expected.

Note that the piece of scintillator used here is approximately square but the smallest face is used for gluing.

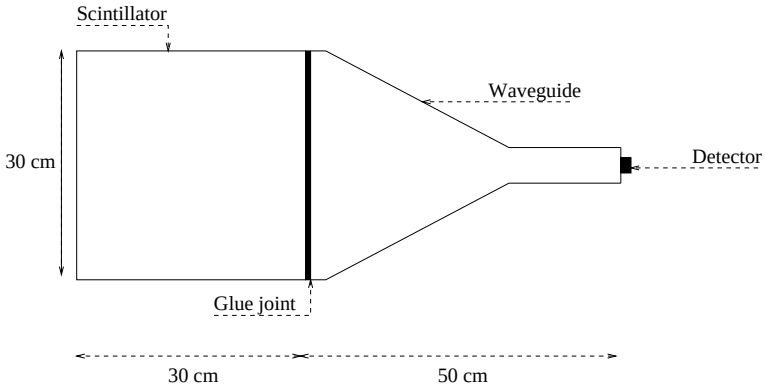

Figure 20: The waveguide readout method

5.3 Readout with a wavelength shifter

This is a commonly used technique for reading out scintillators as the wavelength shifter (WLS) strips are very easy to machine. An added bonus is that the detector can be placed on a small face of the WLS strip, allowing nearly all of the area to be covered. The cotton threads are necessary to provide an air gap which decreases the chance of the WLS light being re-absorbed by the scintillator.

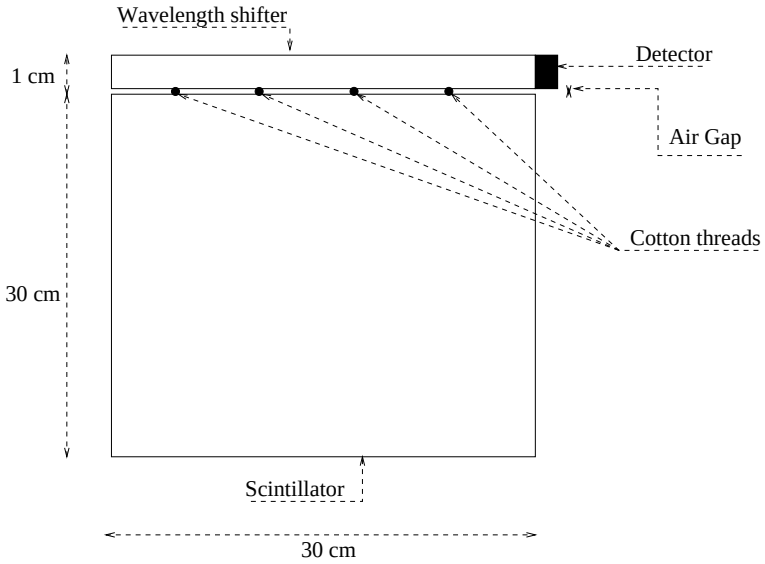

Figure 21: The Wavelength shifter readout method

5.4 Readout with a waveguide and a wavelength shifter

The objective of placing the WLS at the end of the waveguide was to improve the quantum efficiency of the photo-diode and thus increase the detection efficiency. However, it quickly became apparent that the losses incurred due to this further connection would far outweigh any benefits gained by the photo-diode's greater quantum efficiency.

For this reason there were no spectra produced using this method and hence it is omitted from the Results section.

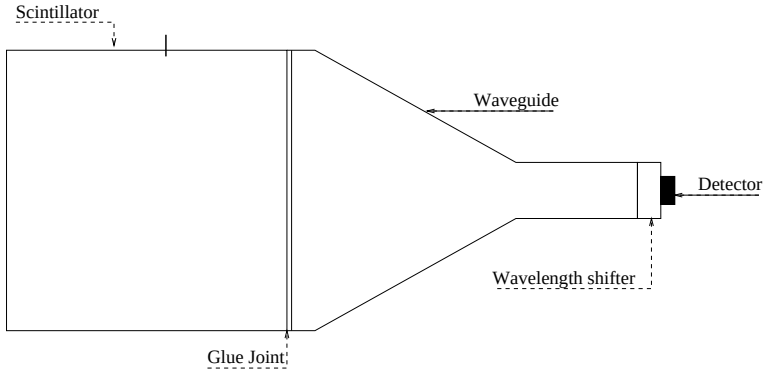

Figure 22: The wavelength shifter and waveguide readout method

6 Results

The nomenclature for the plots of the results is as follows:

- P1 = Amplitude (Number of Counts) of Peak
- P2 = Peak Position (Channel Number)
- P3 = FWHM of the fitted Gaussian

This the standard nomenclature used by the PAW++ Gaussian fitting routine. An estimate of the accuracy of the fit, again using standard nomenclature, is given by the χ^2 per degree of freedom which should, in the case of a good fit, be approximately equal to unity. The PAW++ fitting routine displays:

$$\chi^2/ndf \quad = \quad [\chi^2\, Value]\,/\,[ndf\, Value]$$

where 'ndf' is an abbreviation of Number of Degrees of Freedom. It is left to the reader then to do the simple mathematics! As stressed in Section 4.4.2 the fit used here, a simple gaussian, is not expected to fit the data exactly, but good peak position data is the main aim.

6.1 Calibration

For ease of reference I will include here only the final calibration for the photo-diode and it should also be noted that the H5784 calibration is an **estimate**. Time played a key role in the final stages of the experiment and so absolute calibrations were not done. The justification for this lies in the results themselves, a point I will return to in Section 7.

$$\begin{aligned} \text{2744-08}\ Photo\text{-}diode &\Longrightarrow \quad 1MeV \equiv 23.4\, MCA\ Channels \\ H5784\ Photo\text{-}multiplier &\Longrightarrow \quad 1MeV \cong 80\, MCA\ Channels \end{aligned}$$

Changes in Main Amplifier gain for the H5784 are shown and compensated for appropriately in the relevant sections.

Note that as the gaussian is only used to fit around the peak itself P3 is not an accurate estimate of the error or resolution of the detector. It does however serve as an approximate guide. Also the H5784 is referred to as 'NPM' on the graph simply because that is how I referred to it at that time.

6.2 Photo-diode detection

6.2.1 Direct readout

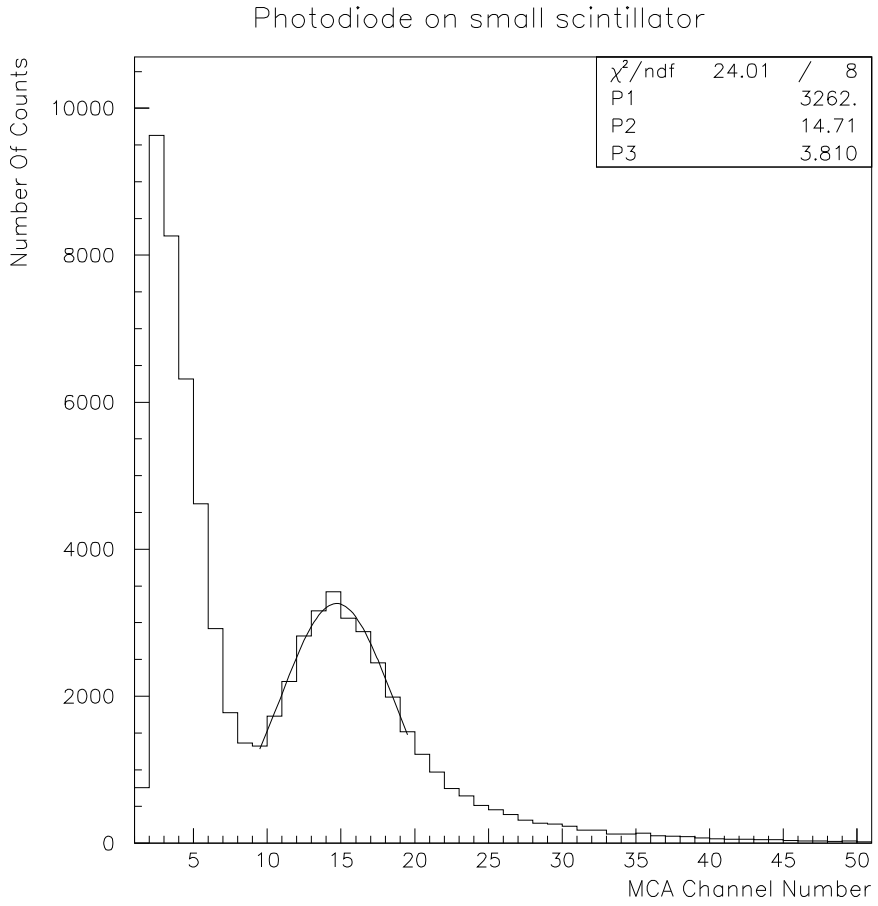

Figure 23: Result of the Direct Readout of a small (10 cm×13 cm) scintillator using a photo-diode

$$\begin{aligned} Peak\,Position &= 14.71\ MCA\ Channels \\ &\Longrightarrow 0.629\ MeV \end{aligned}$$

6.2.2 Readout with a waveguide

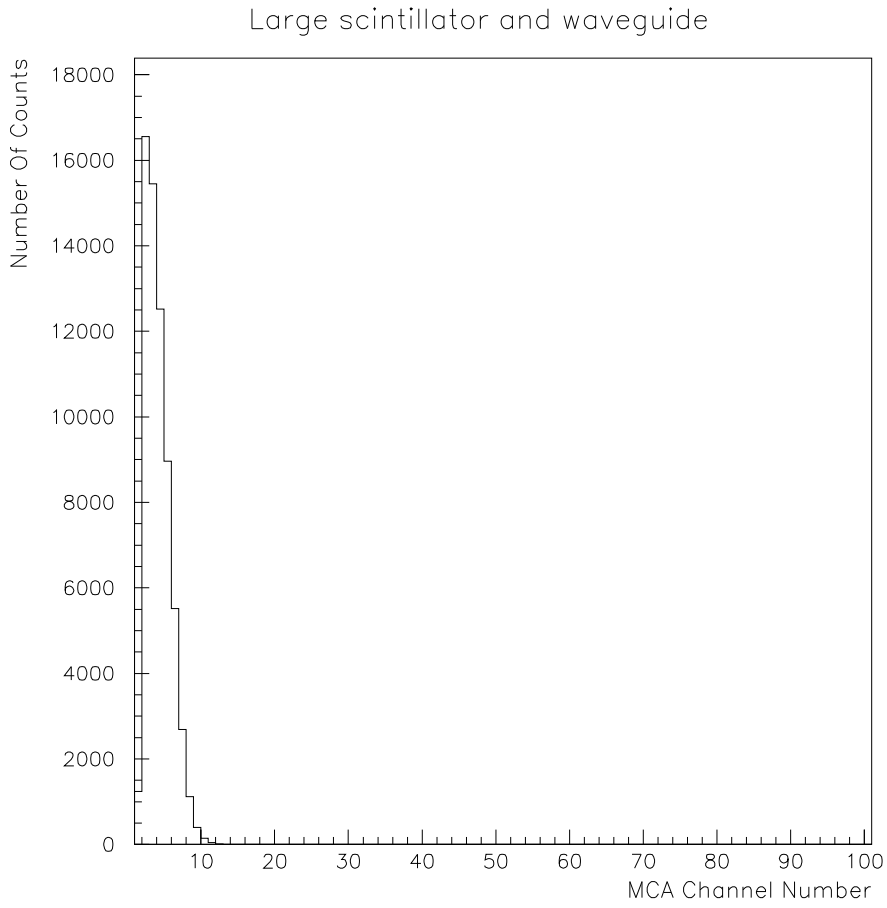

Figure 24: Result of the Readout of a large (30 cm×30 cm) scintillator using a waveguide and a photo-diode

The signal is not discernible from the noise pedestal

6.2.3 Readout with a wavelength shifter

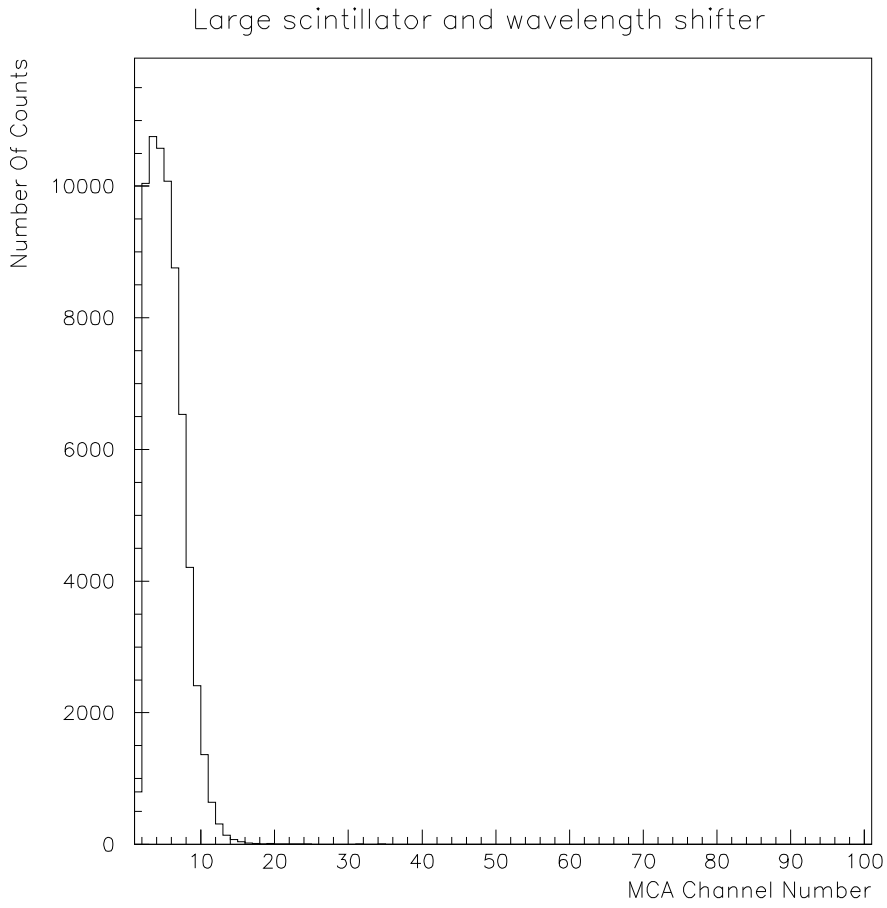

Figure 25: Result of the Readout of a large (30 cm×30 cm) scintillator using a wavelength shifter and a photo-diode

There is evidence of a signal but it is not discernible from the noise pedestal

6.3 Hamamatsu Photo-multiplier detection

6.3.1 Direct readout

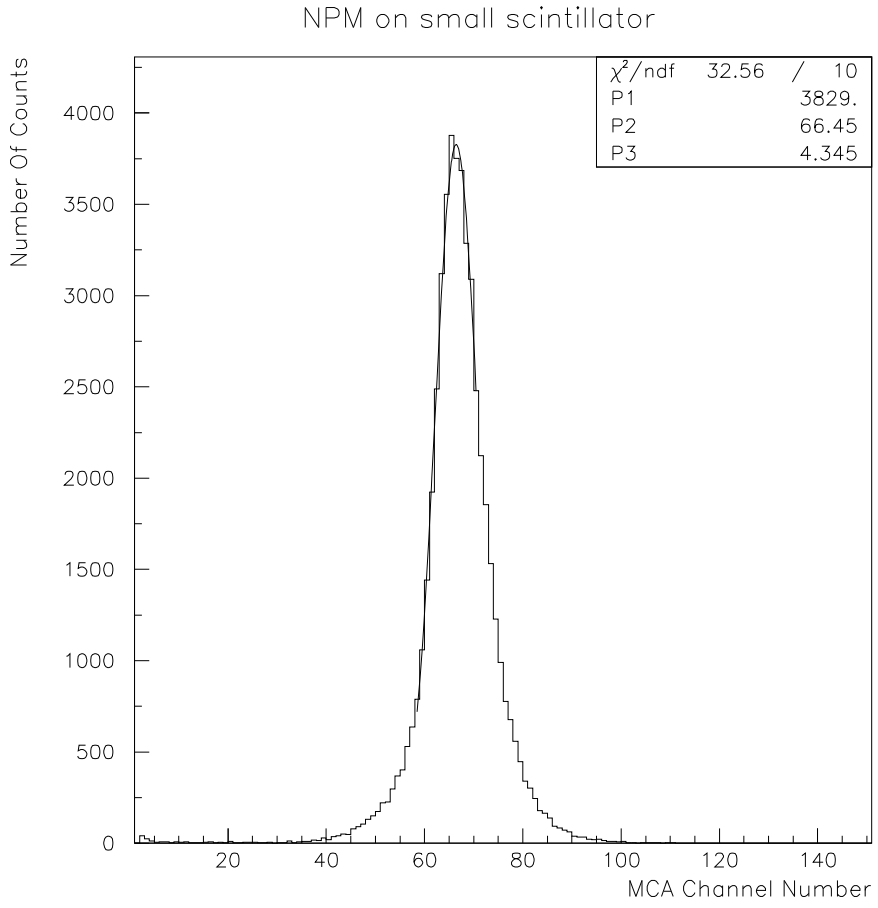

Figure 26: Result of the Direct Readout of a small (10 cm×10 cm) scintillator using the H5784 photo-multiplier

$$\begin{aligned} Peak\,Position &= 66.45\ MCA\ Channels \\ &\Longrightarrow 0.831\ MeV \end{aligned}$$

6.3.2 Readout with a waveguide

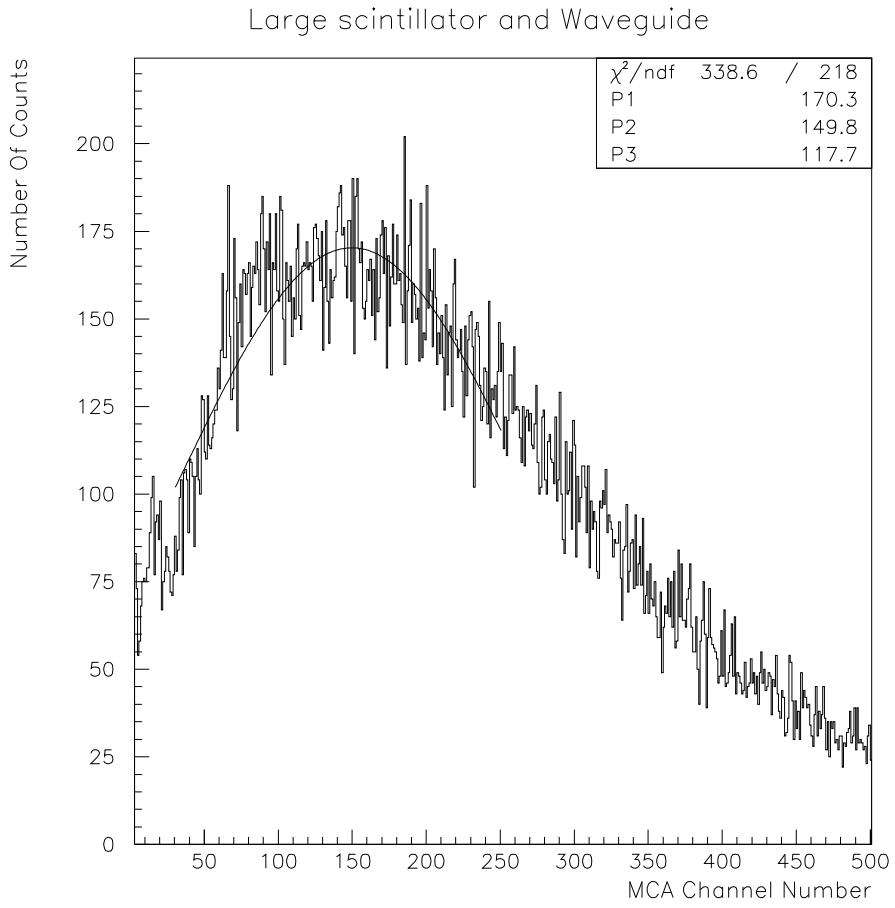

Figure 27: Result of the Readout of a large (30 cm×30 cm) scintillator using a waveguide and the H5784 photo-multiplier

$$\begin{aligned} Gain &= \times 40 \\ Peak\,Position &= 149.8\ MCA\ Channels \\ &\Longrightarrow 0.047\ MeV \end{aligned}$$

6.3.3 Readout with a wavelength shifter

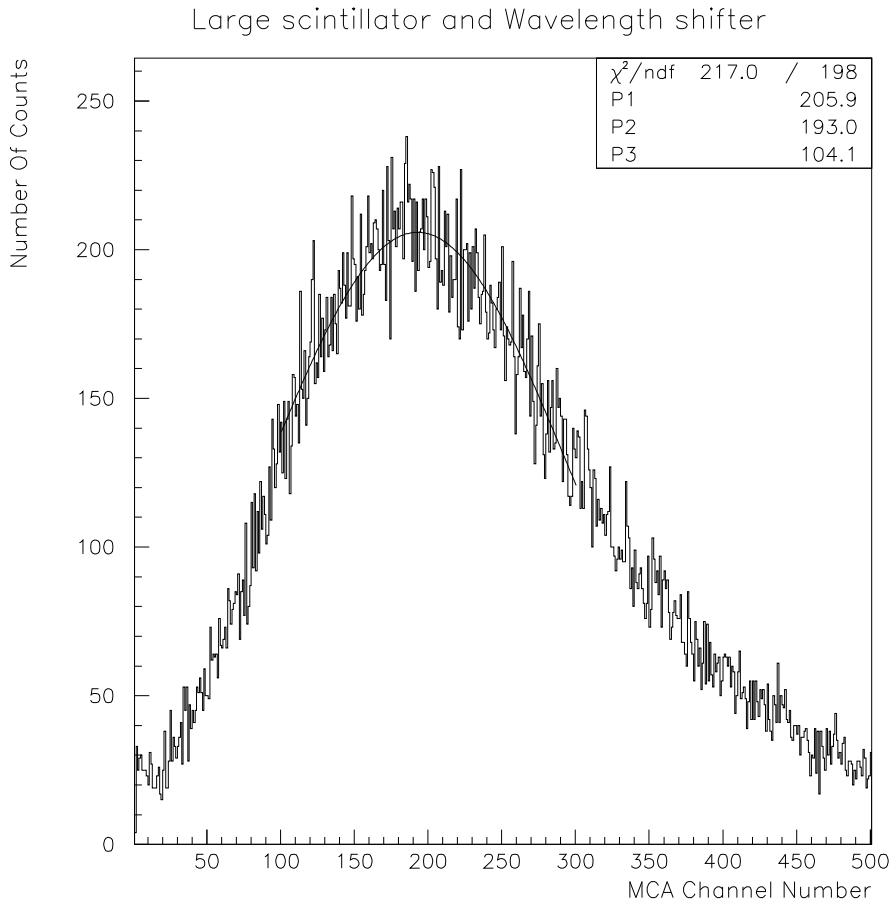

Figure 28: Result of the Readout of a large (30 cm×30 cm) scintillator using a wavelength shifter and the H5784 photo-multiplier

$$\begin{aligned} Gain &= \times 20 \\ Peak\,Position &= 193.0\ MCA\ Channels \\ &\Longrightarrow 0.121\ MeV \end{aligned}$$

7 Conclusions

The conclusions I make here are based mainly on the qualitative comparisons which the results yield. It is for this reason, as well as a lack of time, that I have chosen to ignore the lack of quantitative data, as I believe that the plots in the Results section 'speak for themselves'.

7.1 Comparison of photo-diode with Hamamatsu photo-multiplier

Comparison of Figure 23 (the photo-diode) with Figure 26 (the H5784 photo-multiplier) leads to the immediate conclusion that the H5784 is the superior detector for this purpose. I would also add that the H5784 is far easier to use than the photo-diode as I was able to obtain the spectrum (Figure 26) within a few days of receiving the detector and necessary cables. This should be contrasted with the several months I spent eliminating various noise problems with the photo-diode. Although experience undoubtedly aided me, as I experimented with the photo-diode first, I think that H5784's low-noise characteristics would be of considerable value in the School laboratory.

7.2 Comparison of Combinations

A comparison of Figure 25 with Figure 24 (for the photo-diode) and a comparison of Figure 28 with Figure 27 indicates that the wavelength shifter option would achieve a superior resolution to the waveguide option. In the case of the photo-diode this comparison is based on the wider noise pedestal of Figure 25, an indication that the signal is slightly stronger than the slimmer noise pedestal of Figure 24.

The results of the H5784 experiment show that the signal using the wavelength shifter option (Figure 28) has a greater resolution than the waveguide option (Figure 27). Although there was no absolute calibration of the H5784 Set-up a quantitative comparison between these two spectra is valid and indicates that the wavelength shifter option yields more than twice the energy of the waveguide option.

It should of course be noted that the choice of waveguide length is crucial to any comparison between the two options.

7.3 Overall Conclusions

I conclude that the H5784 is the superior detector for the purposes of the Cosmic Schools Group proposal.

- The H5784 achieves a greater efficiency than the photo-diode
- The H5784 is more suitable for use in the School environment as it is less susceptible to noise than the photo-diode
- A further advantage in terms of teaching is that the H5784 produces cosmic ray signals that are clearly visible on an oscilloscope

The suggested readout technique would be to use a wavelength shifter strip.

7.4 Future Work

The question of the optimum combination of waveguide and wavelength shifter remains unanswered and is likely to require a project of its own. Although this experiment indicates that the wavelength shifter method is the more efficient option it does strictly depend upon the length of waveguide used. The remainder of the questions posed by the Cosmic Schools Group will also require some work, especially as the cost of the H5784, whilst not prohibitive, will place limitations for the cost of the rest of the system.

It is possible that another method of employing the photo-diode could be proposed that would result in an efficient and easy-to-use readout and this is also a possibility for future work. However, I still conclude that the H5784 is by far the most suitable detector for this particular programme.

8 Acknowledgements

I would first of all like to thank Professor Gabathuler for his continued support and enthusiasm throughout this project. I owe much to the early assistance of Dr. Gerd Dahlinger in setting up the telescope and especially for his advice in using the photo-diode. Thanks also to Dave Musket and all of the technical support staff for their prompt delivery of anything I could ask for.

As usual I am very grateful to Dr's Mike Carroll and Christos Touramanis for helping me to use PAW++ and LaTeX, as well as persevering with my descriptions of the seemingly endless 'noise' problems. I am also grateful to everyone else who, at some time or another, popped in to help me get things to work as they should, especially Dr. Steve Biaggi.

9 References

- 'Techniques for Nuclear and Particle Physics Experiments' by W.R.Leo
- 'Particle Physics Booklet' by Particle Data Group
- Notes on the BaBar Experiment:
  - BaBar Note 236 - Performance tests of Hamamatsu 2744-08 diodes for the BaBar calorimeter front end readout and proposal for reliability tests.
  - BaBar Note 216 - Development of the front end readout for the BaBar CsI(Tl) calorimeter
- 'Model 2003BT Silicon Surface Barrier Detector Preamplifier Users Manual' by Canberra
- LaTeX notes supplied by John Milner
- 'PAW Handbook' by CERN Computer Centre

10 Appendices

10.1 Proving that the signal is due to Cosmic Rays

For the sceptic I include here the results of two experiments that I performed with the photo-diode on the small (10 cm×10 cm) scintillator. I also performed these tests with the H5784; a full experiment was not necessary as with the H5784 the cosmic ray signals are clearly visible on an oscilloscope.

The first experiment involved simple placing the detector Scintillator to the side of the two telescope scintillators. A coincidence generated by the telescope should not generate a signal in the detector if the detector is functioning properly.

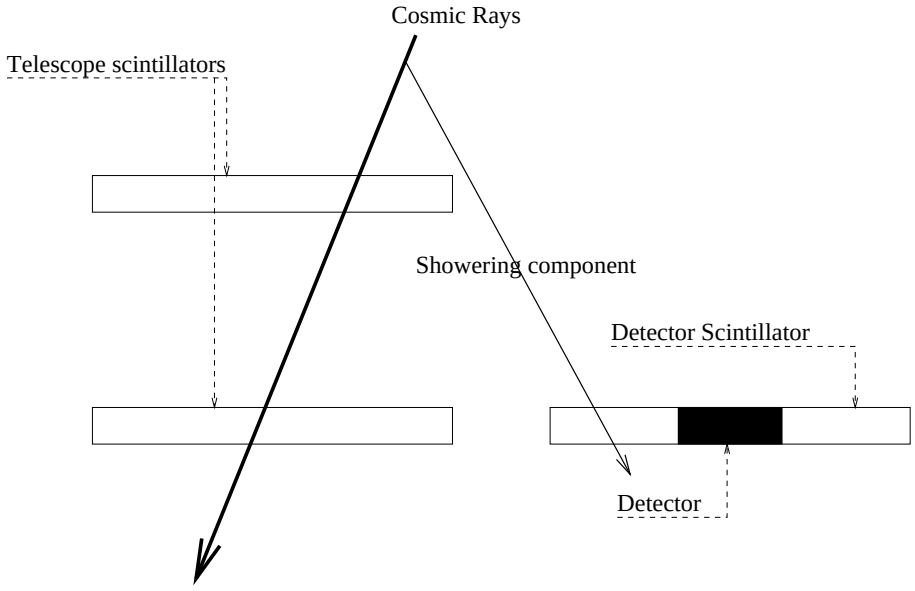

Figure 29: Illustration of the Detector Scintillator placed next to the telescope scintillators

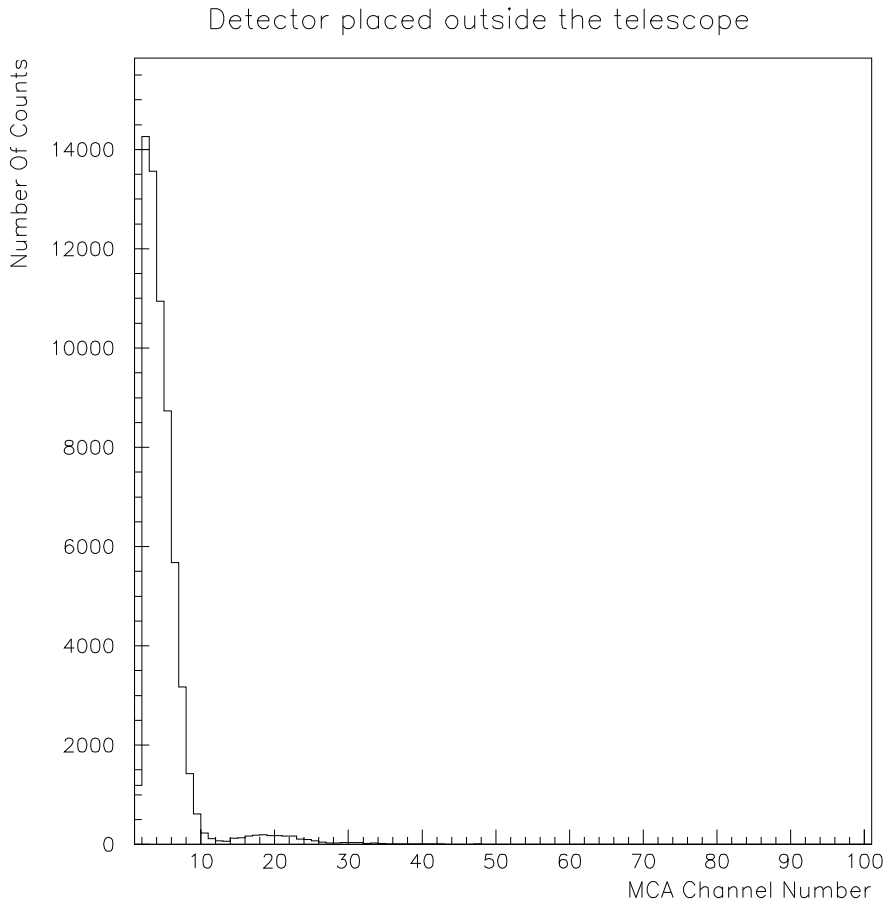

Figure 30: Result of Placing the detector Scintillator outside of the telescope

The most convincing point of this result is that we should not actually expect zero counts generated when a coincidence occurs, as there will be some small fraction of the cosmic rays that will 'shower' through the detector, at the same time as the gate is generated. The small residual peak on the exponential noise background demonstrates this phenomenon and the detector does indeed appear to be detecting cosmic rays.

The second experiment involves simple delaying the telescope trigger long enough so that the generated gate 'misses' the cosmic ray signal in the detector (30μs was used as the gate width used was 15μs). This time there should be no sign of a signal; if the peak remained it must be due to some effect of being placed between the two telescope scintillators.

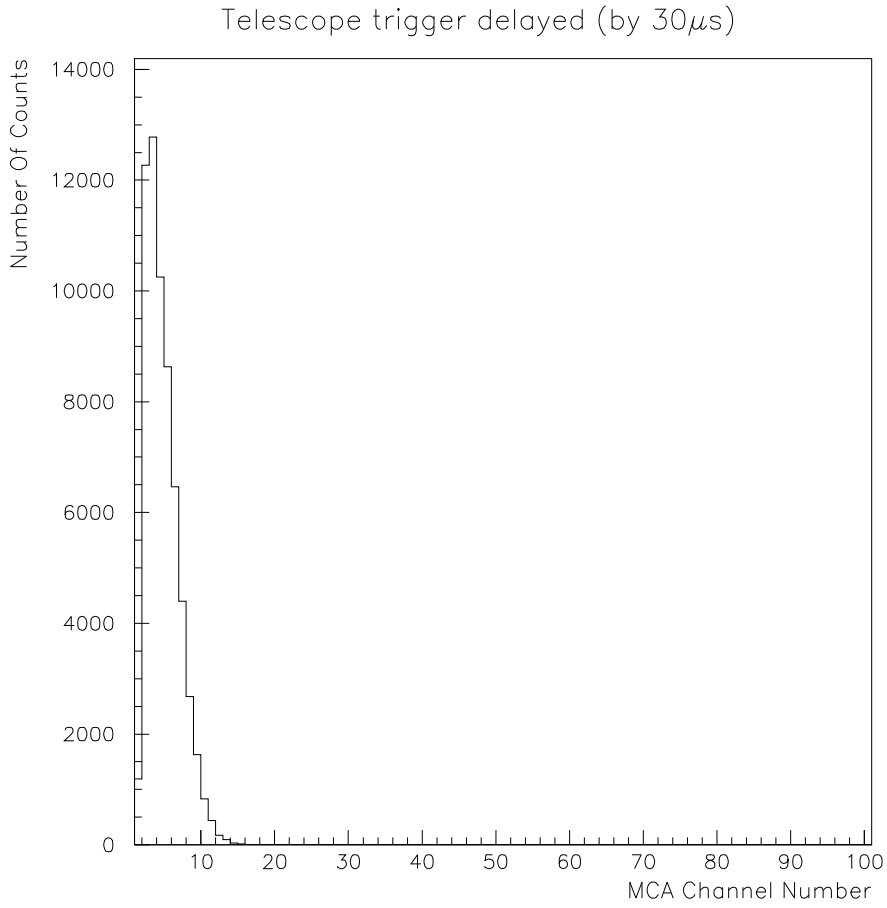

Figure 31: Result of Delaying the Trigger by 30 μs

As expected the signal completely disappears when the trigger is delayed and this, along with the physical behaviour seen in the first experiment, demonstrates that the Set-up functions as a cosmic ray detector.

10.2 Comments on the Resolution

An estimate of the FWHM read from the plot (Figure 26) for the H5784 on the small scintillator is 11 MCA Channels. This converts to a resolution of :

$$\begin{aligned} Resolution &= \frac{11}{66.45} \\ &\simeq 16.5\% \end{aligned}$$

From Section 3.3 we can calculate that, before amplification, we detect 375 photo-electrons ejected from the photo-cathode. The resolution will be given by:

$$\frac{\sqrt{N}}{N} \times 100\%$$

which would give the resolution as $\simeq$ 5 %. However, the resolution we see on the spectrum will be worse than this for two reasons:

1. Degradation occurs as the signal is amplified and processed.
2. There will be a spread in the energy deposition in the scintillators simply because of the flexibility generated by the geometry of the setup. Incoming cosmic rays travel at varying angles, with a strong tendency towards the vertical (usually modelled with a $\cos^2\theta$ dependence) and this variation in angle travelling through the detector Scintillator gives a spread in energy deposition and hence a loss in resolution.

The agreement is good then, especially considering that the experimental result was a first attempt and could presumably be bettered.

The calculations for the photo-diode resolution are not as simple to perform, principally because the noise contribution to the spectrum is significant and must affect the resolution. Clearly the experimental value of $\geq$ 50 % is far greater than the calculation :

$$\begin{aligned} Resolution &= \frac{\sqrt{900}}{900} \\ &\simeq 3.3\% \end{aligned}$$

This initial resolution is quickly degraded on its passage to the preamplifier, despite the good quantum efficiency of the actual device.